ISSN 0006-2979, Biochemistry (Moscow), 2023, Vol. 88, No. 5, pp. 610-620 © Pleiades Publishing, Ltd., 2023.
Published in Russian in Biokhimiya, 2023, Vol. 88, No. 5, pp. 748-760.

Effect of Neurodegenerative Mutations in the *NEFL* Gene on Thermal Denaturation of the Neurofilament Light Chain Protein

Victoria V. Nefedova[1,a]*, Daria S. Yampolskaya[1], Sergey Y. Kleymenov[1,2], Natalia A. Chebotareva[1], Alexander M. Matyushenko[1], and Dmitrii I. Levitsky[1]

[1] *Research Centre of Biotechnology, Russian Academy of Sciences, 119071 Moscow, Russia*
[2] *Koltzov Institute of Developmental Biology, Russian Academy of Sciences, 119334 Moscow, Russia*
[a] *e-mail: victoria.v.nefedova@mail.ru*

Received January 4, 2023
Revised March 2, 2023
Accepted March 2, 2023

Abstract—Effects of E90K, N98S, and A149V mutations in the light chain of neurofilaments (NFL) on the structure and thermal denaturation of the NFL molecule were investigated. By using circular dichroism spectroscopy, it was shown that these mutations did not lead to the changes in α-helical structure of NFL, but they caused noticeable effects on the stability of the molecule. We also identified calorimetric domains in the NFL structure by using differential scanning calorimetry. It was shown that the E90K replacement leads to the disappearance of the low-temperature thermal transition (domain 1). The mutations cause changes in the enthalpy of NFL domains melting, as well as lead to the significant changes in the melting temperatures (T_m) of some calorimetric domains. Thus, despite the fact that all these mutations are associated with the development of Charcot–Marie–Tooth neuropathy, and two of them are even located very close to each other in the coil 1A, they affect differently structure and stability of the NFL molecule.

DOI: 10.1134/S0006297923050048

Keywords: intermediate filaments, neurofilaments, coiled-coil proteins, circular dichroism spectroscopy, differential scanning calorimetry

INTRODUCTION

Intermediate filaments (IF) represent an important component of cytoskeleton, along with microtubules and microfilaments. About 70 genes encoding IF proteins have been described in humans [1, 2]. All proteins of the IF family have similar structural features, in particular, presence of the central α-helical domain (the so-called rod domain). The IF structure is characterized by common structural elements: three α-helical domains (1A, 1B, and 2), which are involved in the formation of coiled-coil domains, are separated by α-helical linkers, which are not involved in the coiled-coil formation [3, 4]. Rod domain of IF is a constituent of the coiled-coil structure and its primary structure is organized as heptad repeats in which amino acid residues are denoted by the letters *a*-*g*. The positions *a* and *d* often contain hydrophobic residues involved in formation of the hydrophobic core, which allows α-helical rod domains to form a coiled-coil structure. IF dimers interact in antiparallel manner and form a tetramer [3, 4]. Assembly of IF from dimers to mature filaments has three stages [5-7]. At the first stage, rapid formation of IF tetramers occurs, next lateral interactions trigger assembly of ULFs (Unit Length Filaments) or protofibrils whose diameter exceeds 10 nm, and, finally, at the last stage, filaments are elongated, compacted, and their diameter is reduced to 10 nm [7]. Principles of the organization of proteins in the IF family

Abbreviations: ΔH_{cal}, calorimetric enthalpy; CD, circular dichroism; DSC, differential scanning calorimetry; IF, intermediate filaments; NFL, NFM, and NFH, neurofilament light, medium and heavy chain proteins; NFL WT, wild type NFL protein; T_m, maximum temperature of thermal transition; ULF, unit length filaments.

* To whom correspondence should be addressed.

are generally universal, but its individual representatives are characterized by unique properties. For example, lamins are not capable of lateral polymerization. Due to complicated organization of the IF protein complexes, point amino acid substitutions even in one domain could lead to serious changes, up to the loss of ability of the mutant protein to self-assembly or to selective blocking of polymerization at the ULF stage (mutation Y117L in vimentin [8]). The most studied members of the IF family are vimentin, desmin and keratins. For them, atomic structures of the coiled-coil domains, including sites responsible for interaction of the dimers and tetramers with each other, have been obtained [3, 4, 9]. Based on the homology between the IFs, it can be assumed that the similar principle of organization would be also characteristic for neurofilaments.

In mature neurons, five IF proteins are expressed – a triad of neurofilament proteins: the neurofilament light (NFL), medium (NFM), and heavy (NFH) chains, as well as peripherin and α-internexin. The main difference between the three neurofilament proteins from each other is determined by their C-terminal domains, which differ both in length and in the presence of important phosphorylation sites. The NFM and NFH proteins are characterized by the presence of long C-terminal domains that contain KSP (Lys-Ser-Pro) repeats that are phosphorylation sites (for example, for Erk 1,2 kinases) [10, 11]. In early studies of the neurofilament structure in neurons, it was shown that the ratio of proteins in the cells is 7/3/2 per NFL/NFM/NFH monomer [10]. Structurally, the proteins are represented by NFL/NFL homodimers, as well as NFL/NFM and NFL/NFH heterodimers [12, 13]. Compared with other IFs, neurofilaments are distinguished by their heterooligomeric structure (heterodimeric), as well as a significant extension along the entire length of the axon, which requires a developed system of their transport. However, *in vitro*, only NFL can self-assembly, while NFM and NFH are not able to polymerize. Formation of the filamentous structures produced by the NFL protein *in vivo* has been shown in the SW13 Vim$^-$ cells that do not express endogenous vimentin [14]. At the same time, NFM and NFH proteins are necessary for the normal expression of NFL in neurons [15].

In this paper, we focused on studying physicochemical properties of the main representative of neurofilaments – the NFL protein. A large number of mutations leading to the development of hereditary Charcot–Marie–Tooth neuropathy (CMT) were found in the *NEFL* gene encoding this protein [16]. This disease includes a group of pathologies that are divided into two types: demyelinating and axonal forms [16, 17]. The first type of neuropathy (CMT 1) is characterized by the decrease in conductivity of the nerve fiber, and the second type (CMT 2) is characterized by the degenerative processes in the axon without reducing the conductivity [18]. The known mutations in the *NEFL* gene can be divided into several groups according to (i) their localization in the structure of the NFL protein or (ii) type of Charcot–Marie–Tooth disease that they cause: demyelinating (1F) or axonal (2E) [17, 19, 20]. Aggregation was demonstrated for a number of the mutant NFL proteins (P8Q, E90K, N98S, A149V) in the cell culture, which in most cases could be eliminated by co-expression of NFL with NFM [21-24]. At the same time, expression of three intermediate filament proteins (NFL, NFM, and peripherin) was necessary to prevent aggregation of the three mutant proteins (N98S, Q332P, E397K) [22]. For the NFL protein with N98S replacement, disruption of assembly and formation of aggregates was shown both in the cell cultures and in the mouse neurons [23]. Moreover, a pronounced tremor and accumulation of aggregates in the cerebellum and spinal cord were observed in the mouse heterozygous N98S/WT model. At the same time, pathological aggregation of the mutant proteins inside the cells was not observed in some studies, but a noticeable decrease in the axon myelinization was detected [25]. Contradictions in the accumulated data raise a number of questions. So, it is not obvious whether formation of the NFL aggregates is a consequence of improper protein folding or is it caused by the changes in its interaction with the protein partners?

Proteins containing amino acid substitutions in the coil 1A (E90K and N98S) and in the coil 1B (A149V) were selected for study in this work (Fig. 1). For these mutant forms of NFL, disruption of assembly (formation of very short filaments or protein aggregates)

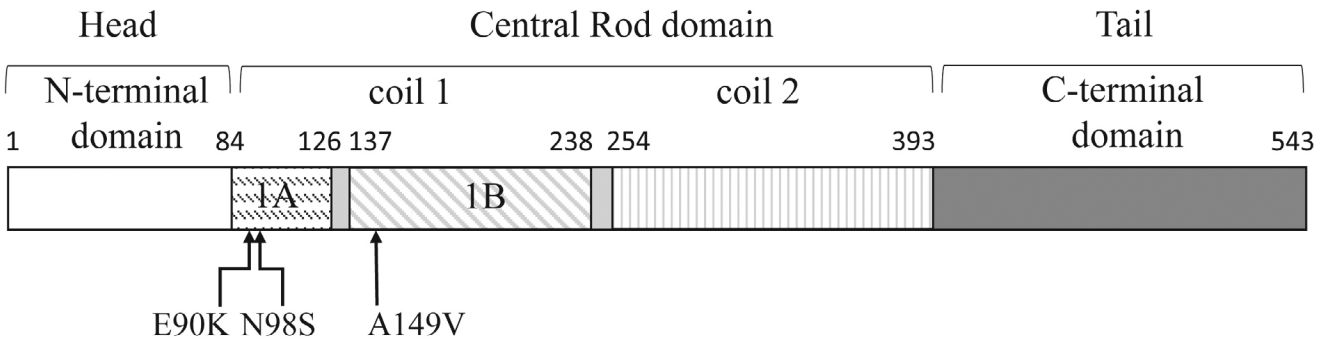

Fig. 1. Structure of the NFL molecule. Arrows mark positions of mutations E90K, N98S, and A149V in the coils 1A and 1B.

was previously shown *in vivo* [21, 22, 24]. To study the causes of pathogenic properties of these NFL mutations, it is necessary to determine effects they have on the protein structure. Position of amino acid residues in the heptads determines structure and properties of the coiled-coil proteins, including stability of the coiled-coil structure, which in turn could affect properties of the NFL oligomers. Considering that the mutations chosen for this study are located in the heptad repeats at positions *d* (E90K), *e* (N98S), and *g* (A149V), i.e., in those positions, which can affect stability of the coiled-coil structure, it can be suggested that the mutations E90K, N98S, and A149V (Fig. 1) may lead to the changes in the coiled-coil structure of the NFL. This assumption is supported by the previously obtained data that the mutations not only at positions *a* and *d* of the heptad repeats, but also at positions *e* and *g* can affect significantly stability (thermal stability) of the coiled-coil of the tropomyosin molecule [26-31]. Verification of this assumption was the main aim of this work. For that, we investigated effects of these amino acid substitutions on thermal denaturation of the NFL protein using circular dichroism (CD) and differential scanning calorimetry (DSC).

MATERIALS AND METHODS

Proteins expression and purification. All NFL protein used in this study were recombinant proteins, products of the human *NEFL* gene (UniProt P07196). Wild-type NFL (WT) and mutant forms were cloned into the EV vector (Cloning Facility, Russia). For introduction of mutations, a Q5-site directed mutagenesis kit (NEB, USA) and the following sets of primers were used. Primers F1 and R1 were used to introduce the N98S substitution; primers F2 and R2 were used to introduce the E90K substitution; primers F3 and R3 were used to introduce the A149V substitution. Sequences of the primer (Evrogen, Russia) are presented in Table 1.

Table 1. Sequences of primers used in this work

Primer	Sequences of primers 5'→3'
F1	GACCTCAGTGACCGCTTCGCCAGCT
R1	CTGGAGCTGCGCCTTCTCCTGCGT
F2	ACGCAGAAGAAGGCGCAGCTCCAGGA
R2	GCGGATGGACTTGAGGTCGTTGCTGA
F3	CTGGTGGCGGAAGATGCCACC
R3	GCGCAGGTCGCGGATCTCCTG

Note. Mutated codons are underlined.

All obtained constructs were used for bacterial expression of proteins in *Escherichia coli* strain C41. Isolation and purification of all recombinant NFL proteins was carried out from the fraction of inclusion bodies. After ultrasonic disintegration of the cells, inclusion bodies were isolated by centrifugation at 18,000*g*. A pellet containing wild type NFL protein (NFL WT) protein or its mutant forms was dissolved in a 20 mM Tris/HCl buffer, pH 8.0, containing 8 M urea, 2 mM EGTA, 15 mM β-ME, 0.1 mM PMSF (buffer A) and subjected to ultracentrifugation at 105,000*g*. Supernatant was loaded onto a HiTrap Q column (GE Healthcare, USA) equilibrated with buffer A. Elution was carried out with a linear NaCl gradient (0-0.7 M NaCl). Protein concentration was determined spectrophotometrically at 280 nm by using extinction coefficient $E^{1\%}$ of 5.9 cm^{-1}. Purified proteins were stored at −80°C. Purity of the obtained preparations was no less than 95% (Fig. 2).

Protein renaturation was performed before the experiments by overnight dialysis against a 5 mM Hepes/NaOH buffer, pH 8.0, containing 0.5 mM EGTA and 2 mM DTT at 4°C.

Analytical ultracentrifugation (AUC). Sedimentation velocity (SV) experiments were carried out in an analytical ultracentrifuge, model E (Beckman, USA), equipped with absorption optics, photoelectric scanner, monochromator, and online computer. Analytical ultracentrifugation was performed at a protein concentration of 1 mg/ml in a 5 mM Tris buffer, pH 8.0, containing 0.5 mM EGTA and 2 mM DTT. An An-G Ti titanium rotor and two-sector cells were used in the experiments. Sedimentation profiles were recorded by measuring

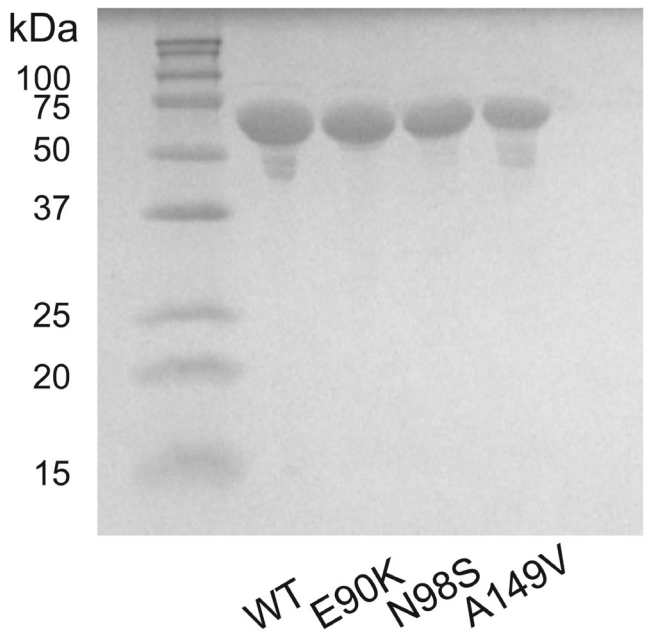

Fig. 2. Analysis of purity of WT NFL and mutants preparations performed by SDS-PAGE.

optical density at 280 nm. All cells were scanned simultaneously with an interval of 2.5 min. Differential distributions of sedimentation coefficients [ls-g*(s) vs s] were determined at 25°C using the SEDFIT program [32].

Circular dichroism spectroscopy (CD). Circular dichroism spectra of NFL proteins were recorded in the range of 190-280 nm at 5°C with a Chirascan CD spectrometer (Applied Photophysics, England) using cuvettes with an optical path length 0.02 cm. Signal registration time for each wavelength was 5 s. At least five CD spectra were recorded for each sample. All experiments were carried out at a protein concentration of 1 mg/ml in a 5 mM Hepes buffer, pH 8.0, containing 0.5 mM EGTA and 2 mM DTT. Temperature dependences of thermal denaturation of proteins were recorded under constant heating rate of 1°C/min in the range 5-85°C at a wavelength of 222 nm.

Differential scanning calorimetry (DSC). DSC experiments were carried out by using a differential scanning microcalorimeter MicroCal VP-Capillary (Malvern Instruments, USA) with capillary measuring cells. Samples were heated at a constant rate of 1°C/min from 10 to 85°C. All experiments were carried out using protein concentration of 2 mg/ml in a 5 mM Hepes buffer, pH 8.0, containing 0.5 mM EGTA and 2 mM DTT. At least three recording were performed for each protein. To study reversibility of denaturation, protein preparations were subjected to two consecutive heatings. Deconvolution procedure, i.e., decomposition of heat absorption curves into separate thermal transitions (calorimetric domains) was carried out with the Origin 7.0 program by fitting data to a model for analysis of multi-domain proteins (a non-two-state model) [33]. This mathematical approach, based on the classical work of Freire and Biltonen [33], was incorporated into the software Origin 7.0 as a "DSC module". This module allows not only deconvolution of DSC curves obtained for the reversibly denaturing proteins, but also a number of other important data processing procedures. For example, it allows to construct (and subsequently subtract from the heat capacity curve) the so-called chemical baseline, connecting the states of native and fully denatured protein. It also makes it possible to accurately determine maximum temperature (T_m) for each thermal transition, and its calorimetric enthalpy (ΔH_{cal}), which represents the integral of excess heat capacity over temperature within the denaturation temperature range of one calorimetric domain or an entire molecule.

RESULTS AND DISCUSSION

NFL protein belongs to the IF family of proteins and has coiled-coil regions which are characteristic for the proteins of this family. However, a distinctive feature of IF proteins is their ability to self-assembly and form various oligomers. For the bovine NFL protein, formation of low molecular weight oligomers (tetramers) was previously shown in a buffer solution with low ionic strength [34]. Sedimentation coefficient of the human NFL WT protein oligomers, obtained under similar conditions by the analytical sedimentation method, was 7.3 S (Fig. 3). Previously, using equilibrium ultracentrifugation, molecular weights of the oligomers of other IFs, vimentin and desmin, obtained under similar conditions [35], were determined. It was shown that at low ionic strength (5 mM Tris-HCl) molecular weight of the oligomers corresponds to tetramers of these proteins. However, sedimentation coefficients of vimentin and desmin tetramers significantly depend on pH, which indicated a different degree of rigidity, size, or shape of the formed oligomers. At pH 8, the sedimentation coefficient of vimentin tetramers was 4.7 S, while at pH 7.5 it was 5.5 S [35]. It was shown in the subsequent work by same authors that the changes in experimental conditions (in particular, increase of protein concentration to 0.5 mg/ml and the addition of EDTA), caused increase of the vimentin sedimentation coefficient up to 7.2 S [36]. This value almost did not differ from the value of 7.3 S determined in our work for the NFL at concentration of 1 mg/ml (Fig. 3).

Taking into account predominance of the main peak 7.3 S in the distribution of ls-g*(s) of NFL WT (Fig. 3), it can be concluded that under the used conditions, this protein was predominantly in the form of oligomers corresponding to tetramers of the NFL protein. Presence of minor amounts of other oligomeric forms with sedimentation coefficients of 5.2, 5.8, or 13.2 S (each form <2%) was also observed. At present, we can only assume that the tetrameric state is also preserved for the mutant forms of NFL (convincing proof of this assumption requires additional experiments, which are planned to be carried out in future).

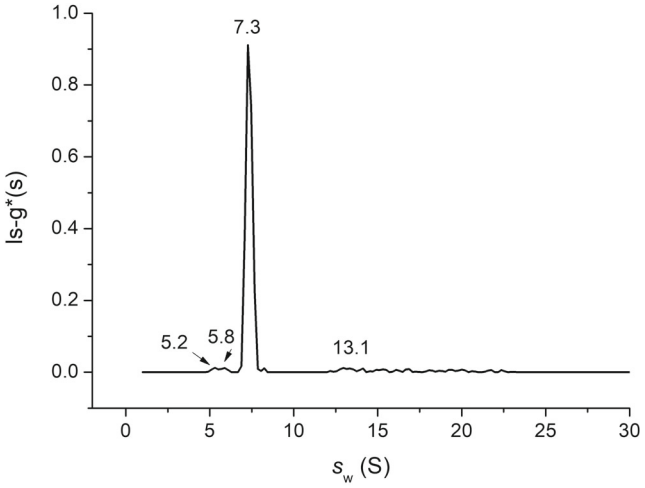

Fig. 3. Analysis of oligomeric state of the NFL WT (1 mg/ml) by analytical ultracentrifugation. Distribution of sedimentation coefficients ls-g*(s) is presented. The rotor speed was 48,000 rpm.

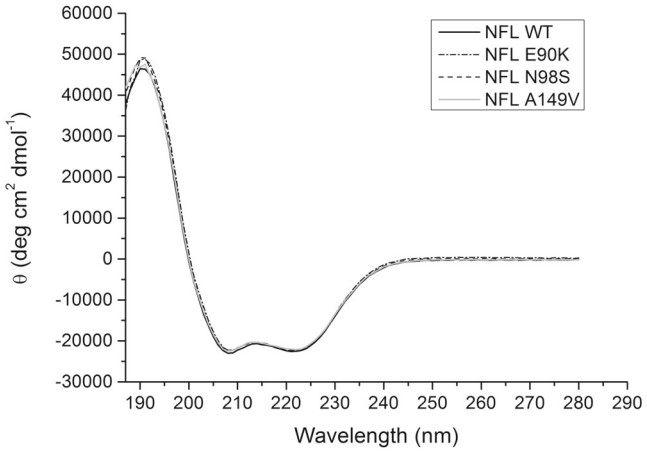

Fig. 4. Circular dichroism spectra of NFL WT and its mutants with substitutions E90K, N98S, and A149V. All spectra were recorded at 5°C.

Nevertheless, we can confidently state that under the used conditions neither NFL WT nor its mutants formed high-molecular-weight oligomers (ULF or filaments), which was confirmed by the complete absence of pellets after high-speed (at 105,000*g*) centrifugation (data not presented). It is important to note that the tetrameric form of IF can exist not only *in vitro*, but also *in vivo* [37], which allows us to consider it as a minimal structure for studying the properties of NFL.

Recorded CD spectra of the WT NFL and all mutant proteins showed presence of the negative maxima of molar ellipticity at 208 and 222 nm, which are characteristic of α-helical proteins (Fig. 4). According to the DichroWeb program (http://dichroweb.cryst.bbk.ac.uk/html/home.shtml), the NFL structure is represented by approximately 52-56% of α-helical regions.

First of all, we studied thermal denaturation of the whole NFL WT molecule and its mutant forms, by monitoring the change in molar ellipticity at 222 nm in the temperature range of 5-85°C (Fig. 5a). It turned out that melting of the NFL WT molecule occurs gradually and has several pronounced thermal transitions (Fig. 5, a-c). By using first derivative of the thermal dependence presented in Fig. 5a, we identified the presence of a thermal transition at ~38°C and a higher

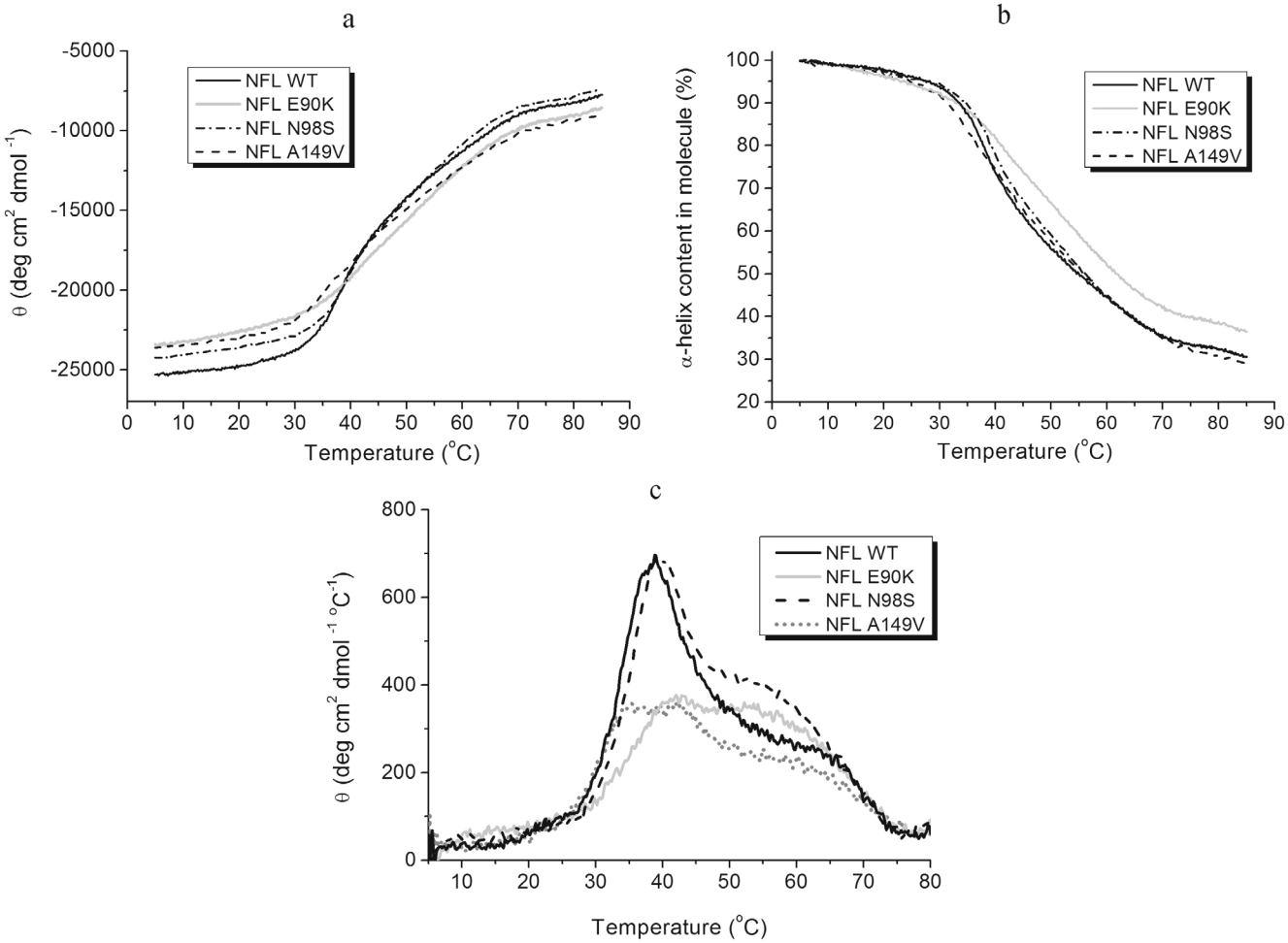

Fig. 5. Thermal denaturation of the NFL WT protein and its E90K, N98S, and A149V mutants, monitored via CD spectroscopy. a) Temperature dependences of molar ellipticity of NFL WT and mutant proteins recorded at 222 nm. b) Temperature dependences of the α-helix content in the NFL molecule. Helicity of the NFL molecule at 5°C, corresponding to ~50% of the protein helicity, was taken as 100%. c) First derivatives of the temperature dependences of ellipticity presented in panel (a).

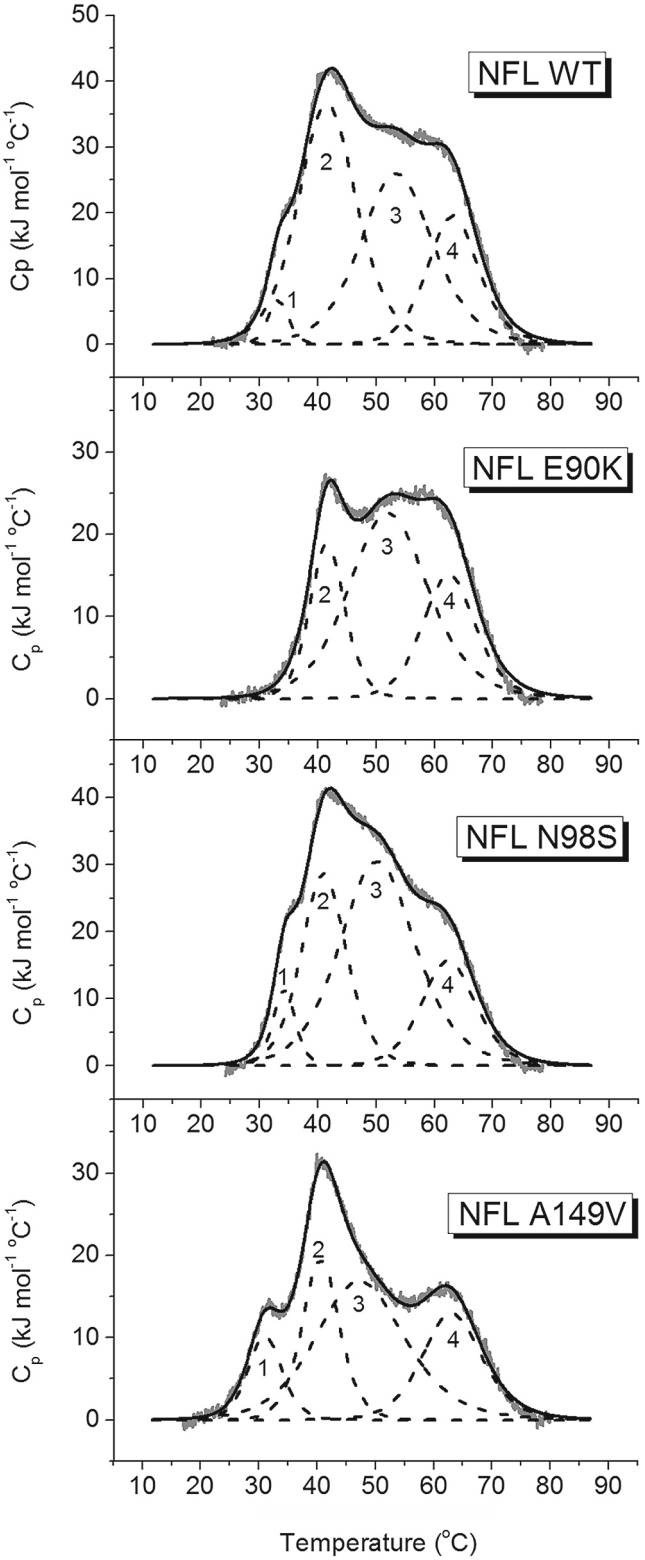

Fig. 6. Temperature dependences of excess heat capacity of the NFL WT protein and its point mutants obtained by DSC. Solid lines show experimental curves of the excess heat capacity, and dotted lines represent calorimetric domains identified by deconvolution of these curves. Numbering of the domains in the figure corresponds to their numbers in Table 2.

temperature "shoulder" (Fig. 5c). Thermal denaturation of the mutant protein with the N98S mutation is very similar to that of the wild-type protein, and also has a pronounced transition at ~39°C. For the mutant protein with the E90K substitution, we found thermal transitions at ~42°C and ~55-57°C. For the NFL protein with the A149V mutation, thermal transitions were detected at ~35°C and ~42°C (Fig. 5c). At the same time, all NFL proteins are characterized by the reversible denaturation. The CD spectra of these proteins after cooling showed the same negative maxima at 208 and 222 nm characteristic for α-helical proteins.

In order to accurately identify thermal transitions in the NFL molecule, we used the DSC method, which allows recording temperature dependences of the excess heat capacity of the protein molecule during its thermal denaturation. NFL melting was completely reversible, which allowed computer-assisted deconvolution of the excess heat capacity curves of the NFL WT and its mutant forms, i.e., decomposition of these curves into separate thermal transitions (calorimetric domains), reflecting denaturation of various protein regions, which melt cooperatively and independently of each other. The obtained data are shown in Fig. 6 and in Table 2.

Based on the results of deconvolution for the WT NFL, 4 calorimetric domains with half-transition temperatures at 33.2°C, 41.7°C, 53.6°C, and 63.2°C were determined. The first derivative graphs of the change in molar ellipticity at 222 nm (Fig. 5c) and the temperature dependences of the excess heat capacity of the WT NFL protein and its mutants (Fig. 6) are, in general, very similar and demonstrate the presence of identical thermal transitions. The CD method makes it possible to register denaturation of the NFL α-helices, while the DSC method detects denaturation of the coiled-coil structure. Similarity of the temperature dependences obtained by these two methods indicates that the destruction of the coiled-coil structure occurs simultaneously with the melting of α-helices.

For all the mutant proteins, except for NFL E90K, 4 calorimetric domains were also identified. The NFL E90K protein did not show any calorimetric domain 1 (Fig. 6, Table 2). It is important to note that, despite the fact that all amino acid substitutions studied in this work are located in coils 1A and 1B (Fig. 1), the changes of calorimetric domains occurred only in the case of one amino acid substitution, E90K. Since this substitution is located in the coil 1A (Fig. 1), it can be assumed that the calorimetric domain 1 reflects denaturation of this region of the NFL molecule. Introduction of other amino acid substitutions (N98S and A149V) changed enthalpy of the individual calorimetric domains, but did not change their number. The smallest changes in the half-transition temperature were observed for the calorimetric domains 2 and 4. For the NFL WT protein and its mutants, the T_m value of calorimetric domain 2

Table 2. Calorimetric parameters obtained by DSC for individual thermal transitions (calorimetric domains) of the wild-type NFL protein and its mutant forms*

NFL	Number of domain	T_m# (°C)	ΔH_{cal}§ (kJ mol^{-1})	ΔH_{cal} (% of total ΔH_{cal})	Total ΔH_{cal} (kJ mol^{-1})
NFL WT	domain 1	33.2	35	3	1190
	domain 2	41.7	495	42	
	domain 3	53.6	430	36	
	domain 4	63.2	230	19	
NFL E90K	domain 2	41.6	150	20	745
	domain 3	52.2	410	55	
	domain 4	62.6	185	25	
NFL N98S	domain 1	34.2	60	6	1080
	domain 2	41.0	295	27	
	domain 3	50.4	530	49	
	domain 4	62.5	195	18	
NFL A149V	domain 1	31.1	80	10	770
	domain 2	40.7	170	22	
	domain 3	47.5	345	45	
	domain 4	63.2	175	23	

Notes. * Parameters were obtained from the data presented in Fig. 6.

Error of the given temperature values of the calorimetric domains (T_m) did not exceed ± 0.2°C.

§ Relative error of the given values of the calorimetric enthalpy (ΔH_{cal}) did not exceed 10%.

is in the range of 40.7-41.7°C, and for the domain 4 – in the range of 62.5-63.2°C. At the same time, introduction of the mutations caused noticeable changes in the calorimetric domain 3. In particular, the T_m value of this domain in the case of the wild-type protein is 53.6°C, while for the mutant protein with the A149V substitution it is much lower, 47.5°C.

The main changes in the thermal denaturation of NFL caused by mutations affect calorimetric domains 1 and 3. To explain possible reasons for the structural changes that may occur upon amino acid substitutions in NFL protein, we examined the structure of IF.

Primary structure of the coil regions of the IF family proteins demonstrates distribution of amino acid residues in the heptad repeats that is typical for all such proteins [26]. In addition, each amino acid residue plays a specific role in stabilization of the coiled-coil structure [26, 38]. For the vimentin protein atomic structures of the individual fragments were previously obtained and distribution of amino acid residues in the coils 1A and 1B was determined (Fig. 7) [3]. Alignment of the primary structures of vimentin and NFL showed that there is high homology between their coils 1A and 1B. Hence, we assumed that the amino acid residues in the heptads of NFL coiled-coil regions would correspond to the same positions (*a*-*g*) as in vimentin. If this is true, then E90 is at position *d*, N98 – at position *e*, and A149 – at position *g* (Fig. 7). The E90K substitution, found in the patients with Charcot–Marie–Tooth neuropathy, leads to disappearance of the calorimetric domain 1 on the NFL thermogram (Fig. 6, Table 2), which may indicate changes in the structure of coil 1A, for example, its higher stabilization or, conversely, destabilization. It was shown, that amino acid positions *a* and *d* of the coiled-coil proteins should contain hydrophobic amino acid residues that stabilize the coiled-coil structure. However, for many intermediate filament proteins (vimentin, glial fibrillar protein, peripherin, desmin), the position homologous to E90 in the NFL also contains an amino acid residue E [3]. At the same time, for the remaining

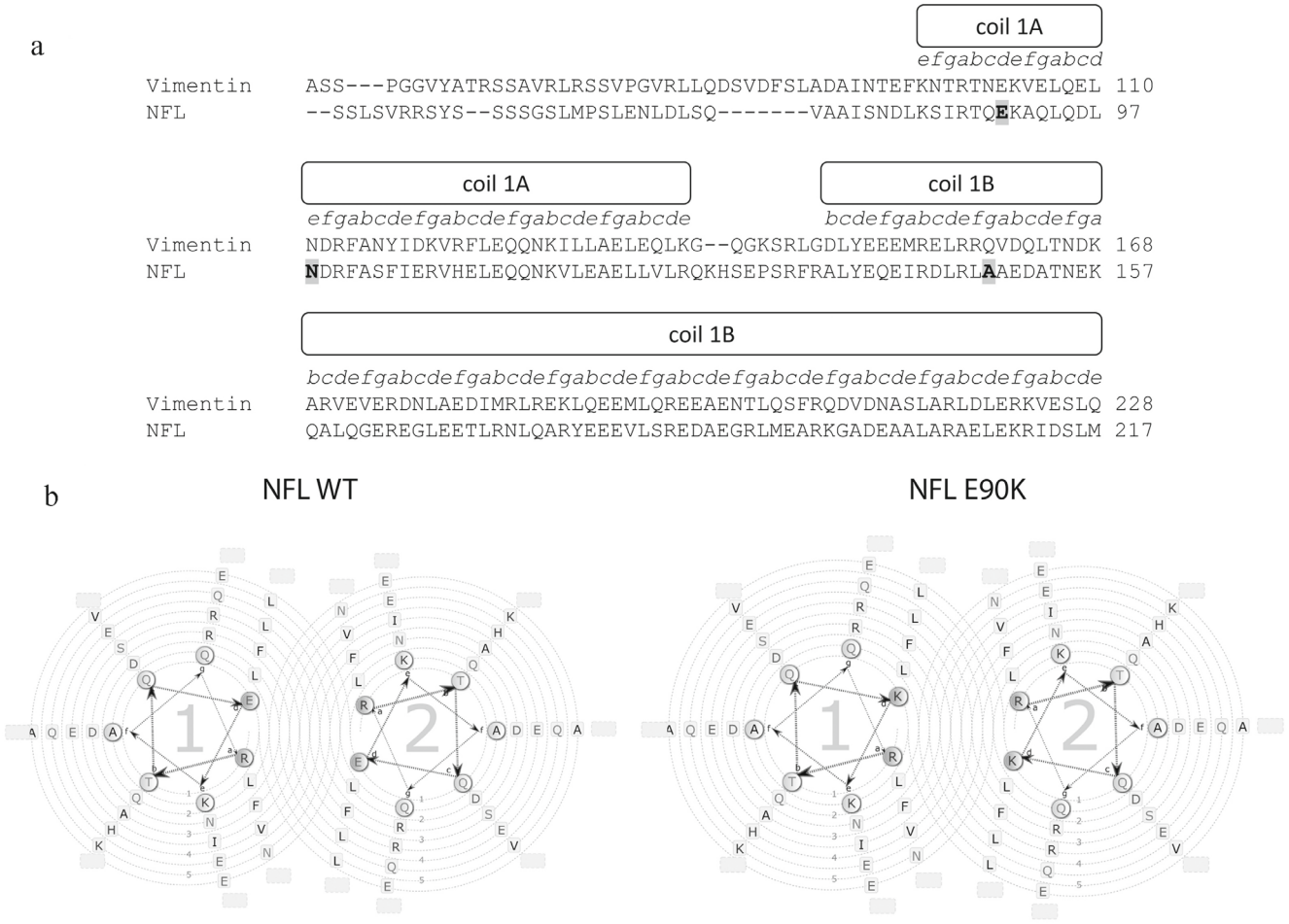

Fig. 7. Analysis of the position of amino acid residues in the heptad repeats of the NFL protein. a) Alignment of primary structures of vimentin (UniProt P08670) and NFL proteins (UniProt P07196). Gray color indicates mutations in the NFL protein that are associated with the development of Charcot–Marie–Tooth neuropathy. Position of amino acids in the heptads is denoted by letters *a-g* and was determined based on the article by Chernyatina et al. [3]. b) Analysis of the position of amino acid residues in the NFL WT and NFL E90K heptads made by using the Waggawagga program [43]. Numbers 1-5 denote various heptads.

residues in the coil 1A, the positions *a* and *d* contain hydrophobic amino acid residues (Fig. 7a). Despite the fact that the E90 amino acid residue is not hydrophobic, it also seems to play an important role in stabilization of the coiled-coil structure of the coil 1A due to electrostatic interactions, since it corresponds to R87 at the position *d* in the hydrophobic core (Fig. 7b). Introduction of the E90K substitution should lead to a local gap between the two α-helices due to appearance of the additional positive charge K90, which causes destabilization of this region in the protein structure. It is important to note that the members of the IF family exhibit capacity to polymerization, and it has been shown in a number of studies that the coil 1A plays an important role in the longitudinal polymerization of IF (i.e., formation of extended filaments). For this coil region of the IF proteins, the lowest melting temperature, ~30°C, was found, and it was suggested that low thermal stability of the 1A coil domain is important for IF polymerization [39-41]. For vimentin, a single amino acid substitution located at the beginning of the linker 1 (K139C) was previously found to cause temperature dependent polymerization. In particular, the protein with the K139C substitution quickly formed ULF both at 21°C and 37°C, however, at 21°C it was not able to form extended fibrils [35]. In this case, it can be expected that the amino acid substitutions that affect thermal stability of NFL could also affect its ability to polymerize. Studies of the NFL E90K mutant polymerization in the SW13 Vim$^-$ cells showed that this protein forms thin short filaments, in contrast to the wild-type protein, which forms long extended filaments under the same conditions [21]. Comparison of these literature data [21] with our results (Fig. 6, Table 2) indicates that the changes in thermal stability induced by the E90K mutation apparently occur in that domain (coil 1A, Fig. 1), which is responsible for NFL polymerization and filament formation.

However, it should be noted, that in the case of IFs, it is also important to take into account their ability for lateral polymerization, which is achieved due to

antiparallel interaction of the dimers. For IF, several types of interactions of dimers in the tetramer were found: A_{11}, A_{12}, and A_{22} [36, 38], which differ in the interacting coils (for example, in the case of A_{11}, the dimers interact antiparallel through the coil 1B). Despite the fact that all three types of interaction are present in the mature IF filament, at the initial stages of polymerization, up to ULF, interaction of the A_{11} type is predominant [35].

Coil 1B plays the main role in the formation of IF tetramers; however, coil 1A and the beginning of coil 2 are also important for the formation of tetramers [3, 42]. This fact can explain the changes in the T_m value of the calorimetric domains 1 and 3, as well as the changes in the enthalpy (ΔH_{cal}) of all calorimetric domains caused by mutations. N98S and A149V mutations led to the changes in the NFL thermal denaturation, however, in both these cases, all four calorimetric domains were retained. This apparently indicates that these mutations do not have such a serious effect on stabilization of the NFL coiled-coil structure. This can be explained by to the fact that these amino acid residues are located in the *e* and *g* positions of the heptad repeats, which are on the surface of coiled-coil structure. Pathogenic properties of these NFL mutations seem to involve disruption of the interaction between the tetramers during formation of ULF and filaments. In particular, aggregation of the NFL N98S protein was previously shown in the SW13 Vim^- cells [21].

CONCLUSION

It can be concluded that point mutations in the NFL protein found in the patients with peripheral Charcot–Marie–Tooth neuropathy do not affect the ability of this protein to form a coiled-coil structure. For all studied mutant proteins with E90K, N98S, and A149V substitutions, presence of the α-helical structure was determined by CD analysis. At the same time, these mutations affect stability and thermal denaturation of the NFL molecule, leading either to the decrease in the number of calorimetric domains detected by DSC, as in the case of the E90K substitution, or to the noticeable changes in the transition temperature (T_m) of the calorimetric domain 3, or to the changes in the calorimetric enthalpy (ΔH_{cal}) of the domains.

In general, the obtained data indicate that the E90K mutation apparently leads to destabilization of the coil 1A in the NFL molecule. As for the N98S and A149V mutations, it can be assumed that they do not affect the coiled-coil structure but might affect other levels of the NFL molecules organization.

Contributions. A.M.M. and V.V.N. – concept and project management; D.S.Y. and V.V.N. – obtaining of NFL preparations; S.Y.K. – performing experiments using DSC method; N.A.C. – conducting experiments using analytical ultracentrifugation method; V.V.N. and D.I.L. – writing the original draft. All authors have read and agreed to the published version of the manuscript.

Funding. The work was financially supported by the Ministry of Science and Higher Education of the Russian Federation, the State Budget Program, projects no. 122041100022-3 (V.V.N., D.S.Y., N.A.C., A.M.M., D.I.L.) and no. 0088-2021-0009 (S.Y.K.).

Ethics declarations. The authors declare no conflicts of interest in financial or any other sphere. This article does not contain any studies with human participants or animals performed by any of the authors.

REFERENCES

1. Herrmann, H., and Aebi, U. (2004) Intermediate filaments: molecular structure, assembly mechanism, and integration into functionally distinct intracellular Scaffolds, *Annu. Rev. Biochem.*, **73**, 749-789, doi: 10.1146/annurev.biochem.73.011303.073823.
2. Kornreich, M., Avinery, R., Malka-Gibor, E., Laser-Azogui, A., and Beck, R. (2015) Order and disorder in intermediate filament proteins, *FEBS Lett.*, **589 (19 Pt A)**, 2464-2476, doi: 10.1016/j.febslet.2015.07.024.
3. Chernyatina, A. A., Nicolet, S., Aebi, U., Herrmann, H., and Strelkov, S. V. (2012) Atomic structure of the vimentin central α-helical domain and its implications for intermediate filament assembly, *Proc. Natl. Acad. Sci. USA*, **109**, 13620-13625, doi: 10.1073/pnas.1206836109.
4. Eldirany, S., Ho, M., Hinbest, A. J., Lomakin, I. B., and Bunick, C. G. (2019) Human keratin 1/10-1B tetramer structures reveal a knob-pocket mechanism in intermediate filament assembly, *EMBO J.*, **38**, e100741, doi: 10.15252/embj.2018100741.
5. Strelkov, S. V., Herrmann, H., and Aebi, U., (2003) Molecular architecture of intermediate filaments, *Bioessays*, **25**, 243-251, doi: 10.1002/bies.10246.
6. Block, J., Schroeder, V., Pawelzyk, P., Willenbacher, N., and Koster, S. (2015) Physical properties of cytoplasmic intermediate filaments, *Biochim. Biophys. Acta*, **1853**, 3053-3064, doi: 10.1016/j.bbamcr.2015.05.009.
7. Herrmann, H., Haner, M., Brettel, M., Ku, N. O., and Aebi, U. (1999) Characterization of distinct early assembly units of different intermediate filament proteins, *J. Mol. Biol.*, **286**, 1403-1420, doi: 10.1006/jmbi.1999.2528.
8. Brennich, M.E., Vainio, U., Wedig, T., Bauch, S., Herrmann, H., and Köster, S. (2019) Mutation-induced alterations of intra-filament subunit organization in vimentin filaments revealed by SAXS, *Soft Matter*, **15**, 1999-2008, doi: 10.1039/c8sm02281j.
9. Lee, C.-H., Kim, M.-S., Li, S., Leahy, D. J., and Coulombe, P. A. (2020) Structure-function analyses of a keratin heterotypic complex identify specific keratin regions

involved in intermediate filament assembly, *Structure*, **28**, 1-8, doi: 10.1016/j.str.2020.01.002.

10. Laser-Azogui, A., Kornreich, M., Malka-Gibor, E., and Beck, R. (2015) Neurofilament assembly and function during neuronal development, *Curr. Opin. Cell Biol.*, **32**, 92-101, doi: 10.1016/j.ceb.2015.01.003.
11. Veeranna, Amin, N. D., Ahn, N. G., Jaffe, H., Winters, C. A., Grant, P., and Pant, H. C. (1998) Mitogen-activated protein kinases (Erk1,2) phosphorylate Lys-Ser-Pro (KSP) repeats in neurofilament proteins NF-H and NF-M, *J. Neurosci.*, **18**, 4008-4021, doi: 10.1523/JNEUROSCI.18-11-04008.1998.
12. Athlan, E. S., and Mushynski, W. E. (1997) Heterodimeric associations between neuronal intermediate filament proteins, *J. Biol. Chem.*, **272**, 31073-31078, doi: 10.1074/jbc.272.49.31073.
13. Garden, M. J., and Eagles, P. A. (1986) Chemical cross-linking analyses of ox neurofilaments, *Biochem. J.*, **234**, 587-591, doi: 10.1042/bj2340587.
14. Sasaki, T., Gotow, T., Shiozaki, M., Sakaue, F., Saito, T., Julien, J.-P, Uchiyama, Y., and Hisanaga, S.-I. (2006) Aggregate formation and phosphorylation of neurofilament-L Pro22 Charcot–Marie–Tooth disease mutants, *Hum. Mol. Genet.*, **15**, 943-952, doi: 10.1093/hmg/ddl011.
15. Yuan, A., Rao, M. V., Julien, J.-P., and Nixon, R. A. (2003) Neurofilament transport In vivo minimally requires hetero-oligomer formation, *J. Neurosci.*, **23**, 9452-9458, doi: 10.1523/JNEUROSCI.23-28-09452.2003.
16. Houlden, H., and Reilly, M. M. (2006) Molecular genetics of autosomal-dominant demyelinating Charcot–Marie–Tooth disease, *Neuromolecular Med.*, **8**, 43-62, doi: 10.1385/nmm:8:1-2:43.
17. Yang, Y., Li-Qiang, Gu, Burnette, W. B., and Li, J. (2016) N98S mutation in NEFL gene is dominantly inherited with a phenotype of polyneuropathy and cerebellar atrophy, *J. Neurol. Sci.*, **365**, 46-47, doi: 10.1016/j.jns.2016.04.007.
18. Rossor, A. M., Polke, J. M., Houlden, H., and Reilly, M. M. (2013) Clinical implications of genetic advances in Charcot–Marie–Tooth disease, *Nat. Rev. Neurol.*, **9**, 562-571, doi: 10.1038/nrneurol.2013.179.
19. Stone, E. J., Kolb, S. J., and Brown, A. (2021) A review and analysis of the clinical literature on Charcot–Marie–Tooth disease caused by mutations in neurofilament protein L, *Cytoskeleton*, **78**, 97-110, doi: 10.1002/cm.21676.
20. Brownlees, J., Ackerley, S., Grierson, A. J., Jacobsen, N. J. O., Shea, K., Anderton, B. H., Nigel Leigh, P., Shaw, C. E., and Miller, C. C. J. (2002) Charcot–Marie–Tooth disease neurofilament mutations disrupt neurofilament assembly and axonal transport, *Hum. Mol. Genet.*, **11**, 2837-2844, doi: 10.1093/hmg/11.23.2837.
21. Perez-Olle, R., Jones, S. T., and Liem, R. K. H. (2004) Phenotypic analysis of neurofilament light gene mutations linked to Charcot–Marie–Tooth disease in cell culture models, *Hum. Mol. Genet.*, **13**, 2207-2220, doi: 10.1093/hmg/ddh236.
22. Stone, E. J., Uchida, A., and Brown, A. (2019) Charcot–Marie–Tooth disease type 2E/1F mutant neurofilament proteins assemble into neurofilaments, *Cytoskeleton (Hoboken)*, **76**, 423-439, doi: 10.1002/cm.21566.
23. Adebola, A. A., Gastri, T. D., He, C.-Z., Salvatierra, L. A., Zhao, J., Brown, K., Lin, C.-S., Worman, H. J., and Liem, R. K. H. (2014) Neurofilament light polypeptide gene N98S mutation in mice leads to neurofilament network abnormalities and a Charcot–Marie–Tooth type 2E phenotype, *Hum. Mol. Genet.*, **24**, 2163-2174, doi: 10.1093/hmg/ddu736.
24. Lee, I.-B., Kim, S.-K., Chung, S.-H., Kim, H., Kwon, T. K., Min, D. S., and Chang, J.-S. (2008) The effect of rod domain A148V mutation of neurofilament light chain on filament formation, *BMB Rep.*, **41**, 868-874, doi: 10.5483/bmbrep.2008.41.12.868.
25. Jordanova, A., De Jonghe, P., Boerkoel, C. F., Takashima, H., De Vriendt, E., Ceuterick, C., Martin, J.-J., Butler, I. J., Mancias, P., Papasozomenos, S. Ch., Terespolsky, D., Potocki, L., Brown, C.W., Shy, M., Rita, D. A., Tournev, I., Kremensky, I., Lupski, J. R., and Timmerman, V. (2003) Mutations in the neurofilament light chain gene (NEFL) cause early onset severe Charcot–Marie–Tooth disease, *Brain*, **126**, 590-597, doi: 10.1093/brain/awg059.
26. Nevzorov, I. A., and Levitsky, D. I. (2011) Tropomyosin: double helix from the protein world, *Biochemistry (Moscow)*, **76**, 1507-1527, doi: 10.1134/S0006297911130098.
27. Nevzorov, I. A., Nikolaeva, O. P., Kainov, Y. A., Redwood, C. S., and Levitsky, D. I. (2011) Conserved noncanonical residue Gly-126 confers instability to the middle part of the tropomyosin molecule, *J. Biol. Chem.*, **286**, 15766-15772, doi: 10.1074/jbc.M110.209353.
28. Kremneva, E., Boussouf, S., Nikolaeva, O., Maytum, R., Geeves, M. A., and Levitsky, D. I. (2004) Effects of two familial hypertrophic cardiomyopathy mutations in α-tropomyosin, Asp175Asn and Glu180Gly, on the thermal unfolding of actin-bound tropomyosin, *Biophys. J.*, **87**, 3922-3933, doi: 10.1529/biophysj.104.048793.
29. Matyushenko, A. M., Shchepkin, D. V., Kopylova, G. V., Popruga, K. E., Artemova, N. V., Pivovarova, A. V., Bershitsky, S. Y., and Levitsky, D. I. (2017) Structural and functional effects of cardiomyopathy-causing mutations in troponin T-binding region of cardiac tropomyosin, *Biochemistry*, **56**, 250-259, doi: 10.1021/acs.biochem.6b00994.
30. Matyushenko, A. M., Artemova, N. V., Sluchanko, N. N., and Levitsky, D. I. (2015) Effects of two stabilizing substitutions, D137L and G126R, in the middle part of α-tropomyosin on the domain structure of its molecule, *Biophys. Chem.*, **196**, 77-85, doi: 10.1016/j.bpc.2014.10.001.
31. Nevzorov, I., Redwood, C., and Levitsky, D. (2008) Stability of two β-tropomyosin isoforms: effects of mutation Arg91Gly, *J. Muscle Res. Cell Motil.*, **29**, 173-176, doi: 10.1007/s10974-009-9171-3.
32. Schuck, P., and Rossmanith, P. (2000) Determination of the sedimentation coefficient distribution by least-

squares boundary modeling, *Biopolymers*, **54**, 328-341, doi: 10.1002/1097-0282(20001015)54:5<328::AID-BIP40>3.0.CO;2-P.

33. Freire, E., and Biltonen, R. L. (1978) Statistical mechanical deconvolution of thermal transitions in macromolecules. I. Theory and application to homogeneous systems, *Biopolymers*, **17**, 463-479, doi: 10.1002/bip.1978.360170212.
34. Nefedova, V. V., Sudnitsyna, M. V., and Gusev, N. B. (2017) Interaction of small heat shock proteins with light component of neurofilaments (NFL), *Cell Stress Chaperones*, **22**, 467-479, doi: 10.1007/s12192-016-0757-6.
35. Mücke, N., Wedig, T., Bürer, A., Marekov, L. N., Steinert, P. M., Langowski, J., Aebi, U., and Herrmann, H. (2004) Molecular and biophysical characterization of assembly-starter units of human vimentin, *J. Mol. Biol.*, **340**, 97-114, doi: 10.1016/j.jmb.2004.04.039.
36. Wickert, U., Mücke, N., Wedig, T., Müller, S. A., Aebi, U., and Herrmann, H. (2005) Characterization of the in vitro co-assembly process of the intermediate filament proteins vimentin and desmin: mixed polymers at all stages of assembly, *Eur. J. Cell Biol.*, **84**, 379-391, doi: 10.1016/j.ejcb.2005.01.004.
37. Soellner, P., Quinlan, R. A., and Franke, W. W. (1985) Identification of a distinct soluble subunit of an intermediate filament protein: tetrameric vimentin from living cells, *Proc. Natl. Acad. Sci. USA*, **82**, 7929-7933, doi: 10.1073/pnas.82.23.7929.
38. Minin, A. A., and Moldaver, M. V. (2008) Intermediate vimentin filaments and their role in intracellular organelle distribution, *Biochemistry (Moscow)*, **73**, 1453-1466, doi: 10.1134/s0006297908130063.
39. Meier, M., Padilla, G. P., Herrmann, H., Wedig, T., Hergt, M., Patel, T. R., Stetefeld, J., Aebi, U., and Burkhard, P. (2009) Vimentin coil 1A – a molecular switch involved in the initiation of filament elongation, *J. Mol. Biol.*, **390**, 245-261, doi: 10.1016/j.jmb.2009.04.067.
40. Vermeire, P.-J., Stalmans, G., Lilina, A. V., Fiala, J., Novak, P., Herrmann, H., and Strelkov, S. V. (2021) Molecular interactions driving intermediate filament assembly, *Cells*, **10**, 2457, doi: 10.3390/cells10092457.
41. Lilina, A. V., Leekens, S., Hashim, H. M., Vermeire, P.-J., Harvey, J. N., Strelkov, S. V. (2022) Stability profile of vimentine rod domain, *Protein Sci.*, **31**, e4505, doi: 10.1002/pro.4505.
42. Premchandar, A., Mücke, N., Poznański, J., Wedig, T., Kaus-Drobek, M., Herrmann, H., and Dadlez, M. (2016) Structural dynamics of the vimentin coiled-coil contact regions involved in filament assembly as revealed by hydrogen-deuterium exchange, *J. Biol. Chem.*, **291**, 24931-24950, doi: 10.1074/jbc.M116.748145.
43. Simm, D., Hatje, K., and Kollmar, M. (2015) Waggawagga: comparative visualization of coiled-coil predictions and detection of stable single α-helices (SAH domains), *Bioinformatics*, **31**, 767-769, doi: 10.1093/bioinformatics/btu700.